Clinical Oral Investigations (2024) 28:97
https://doi.org/10.1007/s00784-024-05489-6

RESEARCH

Effect of a calcium silicate cement and experimental glass ionomer cements containing calcium orthophosphate particles on demineralized dentin

Handially S. Vilela[1] · Rafael B. Trinca[1] · Tarsila V. M. Alves[1] · Tais Scaramucci[2] · Leticia O. Sakae[2] · Flávia S. Mariano[3] · Marcelo Giannini[3] · Flávia R. O. Silva[4] · Roberto R. Braga[1]

Received: 26 October 2023 / Accepted: 3 January 2024 / Published online: 15 January 2024
© The Author(s), under exclusive licence to Springer-Verlag GmbH Germany, part of Springer Nature 2024

Abstract

Objective The study aims to evaluate the effect of a glass ionomer cement (GIC; Fuji 9 Gold Label, GC) with added calcium orthophosphate particles and a calcium silicate cement (CSC; Biodentine, Septodont) regarding ion release, degradation in water, mineral content, and mechanical properties of demineralized dentin samples.

Methods GIC, GIC + 5% DCPD (dicalcium phosphate dihydrate), GIC + 15% DCPD, GIC + 5% β-TCP (tricalcium phosphate), GIC + 15% β-TCP (by mass), and CSC were evaluated for Ca^{2+}/Sr^{2+}/F^{-} release in water for 56 days. Cement mass loss was evaluated after 7-day immersion in water. Partially demineralized dentin disks were kept in contact with materials while immersed in simulated body fluid (SBF) at 37 °C for 56 days. The "mineral-to-matrix ratio" (MMR) was determined by ATR-FTIR spectroscopy. Dentin hardness and elastic modulus were obtained by nanoindentation. Samples were observed under scanning and transmission electron microscopy. Data were analyzed by ANOVA/Tukey test ($\alpha = 0.05$).

Results Ca^{2+} release from CSC and GIC (μg/cm^2) were 4737.0 ± 735.9 and 13.6 ± 1.6, respectively. In relation to the unmodified GIC, the addition of DCPD or β-TCP increased ion release ($p < 0.001$). Only the dentin disks in contact with CSC presented higher MMR ($p < 0.05$) and mechanical properties than those restored with a resin composite used as control ($p < 0.05$). Mass loss was similar for GIC and CSC; however, the addition of DCPD or β-TCP increased GIC degradation ($p < 0.05$).

Conclusion Despite the increase in ion release, the additional Ca^{2+} sources did not impart remineralizing capability to GIC. Both unmodified GIC and CSC showed similar degradation in water.

Clinical relevance CSC was able to promote dentin remineralization.

Keywords Dentin remineralization · Calcium silicate · Calcium orthophosphate · Glass ionomer cement

Introduction

Minimally invasive restorative approaches advocate the removal of the necrotic, infected dentin layer and the sealing of the cavity margins [1, 2] in order to reduce the number and diversity of bacteria and interrupt of the carious process [3–6]. Clinical evidence indicates that the effective sealing of the cavity walls is more important for the success of the minimally invasive therapy than the use of materials capable of stimulating reactional tertiary dentin formation [7–9]. Notwithstanding, calcium-releasing materials have been shown to be effective in dentin remineralization [10] and could increase process efficiency.

Calcium silicate (CSC) cements release Ca^{2+} and OH^{-} ions in levels capable of fostering apatite precipitation in contact with physiological fluids. In recent years, their indications expanded

✉ Roberto R. Braga
rrbraga@usp.br

[1] Department of Biomaterials and Oral Biology, School of Dentistry, University of São Paulo, Av. Prof. Lineu Prestes, 2227, São Paulo, SP 05508-000, Brazil

[2] Department of Restorative Dentistry, School of Dentistry, University of São Paulo, São Paulo, Brazil

[3] Department of Restorative Dentistry, School of Dentistry, University of Campinas, São Paulo, Brazil

[4] Institute of Energy and Nuclear Research, University of São Paulo, São Paulo, Brazil

considerably, including as remineralizing materials applied on caries-affected dentin [11–13]. In fact, samples of demineralized dentin in contact with a CSC showed an increase in mineral content up to 50-µm depth after 30 days in phosphate-containing solution [14]. Biodentine (Septodont, St-Maur-des-Fossés, France) is a calcium silicate-based cement with improved mechanical properties due to a less porous microstructure, indicated for long-term temporary restorations [15, 16].

Considered the first option in minimally invasive restorative procedures due to the ability to adhere to dental structures [17], glass ionomer cement (GIC) potential to promote mineral gain in demineralized dentin has been challenged [18, 19]. Its acidity promotes the dissolution of dentin hydroxyapatite, which can re-precipitate as calcium fluoride, fluorapatite, or fluoridated hydroxyapatite. Thus, GIC would promote mineral exchange for a more acid-resistant phase, but no effective mineral gain [20].

The addition of calcium sources to GIC as a way to increase its remineralization potential has been evaluated [21–25]. Among the possible calcium sources that can be incorporated into the GIC, calcium orthophosphates (CaP), a group of compounds with distinct chemical structures ("phases"), have been tested [21]. However, although studies report an overall increase in ion release, there are no reports on the actual effect of these CaP-modified GICs on dentin remineralization.

Direct comparisons between GIC (unmodified) and CSC on dentin remineralization have been reported, but without consensus among authors [19, 26–29]. Though disagreements can be attributed to methodological differences, it is worth mentioning that most investigations used qualitative evaluations, and only one study focused on the mechanical properties of demineralized dentin specimens, showing superior results for CSC [19].

Considering the above, the objective of the present study was to evaluate the remineralization ability of a calcium silicate cement and a glass ionomer cement modified by the addition calcium orthophosphate particles. Additionally, the materials were tested for ion release and degradation in water. The null hypotheses were (1) the substitution of GIC glass by DCPD or β-TCP particles does not affect the cement's ion release or degradation in water, (2) GIC (either unmodified or modified) present similar Ca^{2+} to CSC, and (3) GIC (either unmodified or modified) and CSC show similar effects on mineral content and mechanical properties of demineralized dentin.

Materials and methods

Materials

Fuji Gold Label 9 (GC Corporation, Tokyo, Japan) and Biodentine (Septodont, St-Maur-des-Fossés, France) were used in all experiments. For the ionomeric cement, the proportion 3.6 g of particles:1.0 g of liquid was followed, as per manufacturer recommendation. The mixture was made for 30 s on a glass slab using a plastic spatula. In four experimental groups, at each manipulation, 5% or 15% of GIC particles mass was replaced by either DCPD or β-TCP. The replacement of glass particles by either additive was made prior to each manipulation in order to avoid variability among samples due to inhomogeneous distribution. Biodentine was mechanically mixed for 30 s, as per manufacturer recommendation. In dentin remineralization evaluations (mineral:matrix ratio, nanoindentation, SEM, and TEM), a resin-based composite (Filtek Z250, 3 M ESPE, St. Paul, MN, USA) was used as negative control.

DCPD and β-TCP synthesis and characterization

DCPD particles were synthesized by precipitation, using calcium nitrate tetrahydrate ($Ca(NO_3)_2.4H_2O$) and ammonium dihydrogen phosphate ($(NH_4)H_2PO_4$) solutions as precursors (both reagents purchased from Sigma-Aldrich, St. Louis, USA), both at 0.25 mol/L. The receptor solution (containing the phosphate ions) had its pH stabilized at 5.0 and the synthesis was conducted at room temperature (22 ± 2 °C). At the end of the drop-wise mixture, the solution remained under magnetic stirring for 15 min, followed by the filtration, rinsing (two cycles in deionized water and two cycles in absolute ethanol), and vacuum-drying [30]. β-TCP particles were also synthesized by the precipitation, using precursor solutions of H_3PO_4 (0.3 mol/L), calcium hydroxide ($Ca(OH)_2$), and magnesium hydroxide ($Mg(OH)_2$; 0.5 mol/L) (all reagents acquired from Synth Ltda, Diadema, Brazil). After precipitation, the solution was filtered and rinsed in ultrapure water. After drying at 60 °C overnight, particles were heat-treated at 1000 °C for 30 s using an adapted microwave oven [31].

Phase formation was confirmed by X-ray diffractometry (Multiflex, Rigaku Corp., Tokyo, Japan). Particle size distribution was determined by laser light scattering (Mastersizer 2000, Malvern, Instruments Ltd., Malvern, UK) and their morphologies were observed under scanning electron microscopy (JEOL, model 1010, Tokyo, Japan).

Cement microstructure and elemental composition

Disks (5×1 mm, $n = 3$) of the six evaluated cements were prepared. After 24 h at 37 °C and 100% relative humidity, they were embedded in acrylic resin polished with sandpaper grits #800, #1000, #1500, #2000, #3000, #4000 and carbon-coated for observation under the scanning electron microscope (JEOL, model 1010) equipped with an energy-dispersive X-ray spectroscopy system (Bruker

Xflash 4030 with detector SDD—Silicon Drift Detector, MA, USA). The calcium percentages in the set cements were calculated based on the powder:liquid ratio and the elemental composition of DCPD, β-TCP, Biodentine, and GIC glass particles obtained by X-ray fluorescence spectroscopy (Zetium, Malvern Panalytical).

Mass loss in water

Cement disks (5 × 1 mm, $n = 3$) were prepared and kept dry for 15 min. After having their initial mass determined on an analytical balance (Mettler Toledo, model XS105, Columbus, OH, USA), the specimens were immersed in 5 mL of deionized water at 37 °C. After 7 days, the specimens were transferred to an open Eppendorf and kept in an oven at 105 °C until no change in mass was observed [32].

Calcium, strontium, and fluoride release

Calcium (for GICs — both unmodified and modified with CaP particles — and Biodentine) and strontium release (only for GICs) were quantified by induced coupled plasma optical emission spectroscopy (ICP-OES; Agilent Technologies, Santa Clara, USA). Disks (5 × 1 mm, $n = 3$) were kept at room temperature for 15 min [33] and then individually immersed in 5 mL of deionized water (DW). After 24 h, 14, 28, 42, and 56 days, disks were transferred to new tubes containing fresh DW. The solutions were filtered (pore size: 0.45 µm) and acidified with 5 µL of 100% nitric acid prior to the analysis. Fluoride release from unmodified and modified GICs was determined using an ion-specific electrode (Orion Research, Boston, MA, USA) [34]. Equal volumes of immersion medium and TISAB II were mixed and the values compared with a standard curve. In both assays, the results were obtained in parts per million (ppm) and converted to µg/cm^2.

Dentin remineralization

Demineralization procedure

Extracted third molars were collected according to the Ethics Committee standards of the institution and stored at − 20 °C for up to 90 days before use. Dentin disks (3-mm thick) were prepared using a metallographic saw (Isomet 1000, Buehler, Rochester Hills, USA) equipped with a high-concentration diamond disk, under refrigeration. The occlusal surface was polished with sandpaper granulations #800, #1200, #1500, #2000, #2500, #3000, and #4000. The opposite surface and the lateral surface were protected with cosmetic varnish. The disks were immersed in a solution containing 2.2 mmol L^{-1} calcium phosphate and 0.05 mmol L^{-1} acetic acid adjusted to pH 5.0 with NaOH pellets for 66 h at room temperature, under stirring [35].

Mineral:matrix ratio (ATR-FTIR spectroscopy)

The variation in dentin mineral content at the interface with the restorative material was determined by mid-infrared spectroscopy (Vertex 70, Bruker Optics GmbH, Germany) using an attenuated total reflectance accessory with a diamond crystal (ATR-FTIR, Miracle, Pike Technologies, Inc., Madison, WI, USA). Since this is a non-destructive analysis, the same specimens were analyzed before and after demineralization, and every 14 days for 56 days. Disks (8 × 2 mm, $n = 5$) of the restorative materials were previously prepared and kept in contact with the demineralized dentin surface through a dental floss tie. The specimens were individually immersed in tubes containing 10 mL of simulated body fluid (SBF) and kept at 37 °C for 56 days [36]. The SBF solution was changed weekly. Spectra ranging between 400 and 4000 cm^{-1} at a resolution of 8 cm^{-1}, using 32 scans per spectrum were collected at three different areas of the dentin surface. The area of the bands corresponding to phosphate (υ_3PO_4; i.e., O–P–O bonds in the asymmetrical elongation mode: 885 to 1180 cm^{-1}) and amide bonds present in type I collagen (− CNH or C = O: 1200 cm to 1725 cm^{-1}) were used to calculate the "phosphate:amide II" or "mineral-to-matrix" (MMR) ratio [37]. Variations in MMR in relation to the demineralized (initial) condition were used as an estimate of dentin mineral gain at the interface with the restorative material.

Dentin hardness and elastic modulus (nanoindentation)

The materials were applied directly on the demineralized dentin and the specimens ($n = 10$) were stored in SBF at 37 °C (changed weekly) for 56 days. After the storage period, the samples were sectioned transversely in 1-mm-thick slices, which were included in acrylic resin and polished in sandpaper grit #800 to #4000. Dentin hardness and elastic modulus were evaluated in an ultramicrodurometer (Dynamic Ultra Micro Hardness Tester DUH-211S, Shimadzu, Kyoto, Japan) with a Berkovich indenter (tip angle: 115°, tip radius: 0.1 µm). Indentations (5 mN for 5 s) were made following three lines perpendicular to the restoration-dentin interface, each with 14 indentations with a spacing of 15 µm between each indentation, from the restoration-dentin interface to the sound dentin, extending through the entire depth of the lesion [38].

Scanning electron microscopy

Two randomly selected specimens analyzed in ATR-FTIR spectroscopy were carbon-coated and observed under a scanning electron microscope (SEM; JEOL, model 1010, Tokyo, Japan).

Transmission electron microscopy

Slices (1 mm in thickness) of two randomly selected specimens tested for nanoindentation analysis were processed for observation under transmission electron microscopy. The slices were fixed in Karnovsky fixative, post-fixed in 1% osmium tetraoxide, dehydrated in increasing concentrations of ethanol (30–100%), immersed in propylene oxide, and embedded in epoxy resin. Sections with thickness between 50 and 60 nm were obtained in a ultramicrotome, collected on copper grids, and observed under 80 kV (Philips CM12; Philips, Eindhoven, The Netherlands).

Statistical analysis

Mass loss and cumulative, 56-day ion release data were submitted to one-way ANOVA/Tukey test. ATR-FTIR spectroscopy, nanohardness, and elastic modulus data were analyzed using repeated measures two-way ANOVA/Tukey test. Statistical power for each test was at least 0.96 (Statistica 14.0, TIBCO Software, Inc.). In all cases, the significance level of 5% was adopted.

Results

DCPD and β-TCP particle characterization

Particle size medians (D_{50}) were 22 µm for DCPD and 11 µm for β-TCP. DCPD particles presented as large, smooth plates with rounded corners, whereas β-TCP particles are spherical nanoparticle clusters (Fig. 1).

Cement microestrututcture

The cement microstructures are shown in Fig. 2. The GIC glass particles (blue) appear surrounded by the cement matrix. Calcium orthophosphate particles are observed in orange. GICs containing 15% of DCPD show smaller glass particles (consequently, a higher matrix fraction) and larger cracks (formed during sample processing) compared to the unmodified GIC and the materials with 5% DCPD or β-TCP. The CSC also has zirconium in its composition, represented in yellow. Like the GICs, it has pores; however, it has no visible cracks.

The calcium percentages (by mass) in the set cements were 0.1% (GIC), 1.9% (GIC + 5% DCPD), 2.1% (GIC + 5% β-TCP), 9.5% (GIC + 15% DCPD), and 10.5% (GIC + 5% β-TCP). For the set CSC, the calcium percentage was 55.4%.

Mass loss in water

GIC and CSC showed similar mass loss (11.0 ± 1.0% and 9.1 ± 0.4%, respectively; Fig. 3). The addition of 15% β-TCP resulted in a statistically higher degradation in relation to the unmodified GIC ($p > 0.05$).

Calcium, strontium, and fluoride release

Non-cumulative ion release curves are shown in Fig. 4. Only the GIC modified with 15% DCPD showed a higher release at 24 h compared to the other periods. Overall, the presence of additives increased ion release in relation to the unmodified GIC ($p < 0.05$; Table 1). Considering the cumulative Ca^{2+} release from CSC was several times higher than the release from the GICs, it was not included in the statistical analysis. CSC showed a much higher release in the first 24 h (1933 µg/cm^2), compared to the subsequent periods (112–501 µg/cm^2).

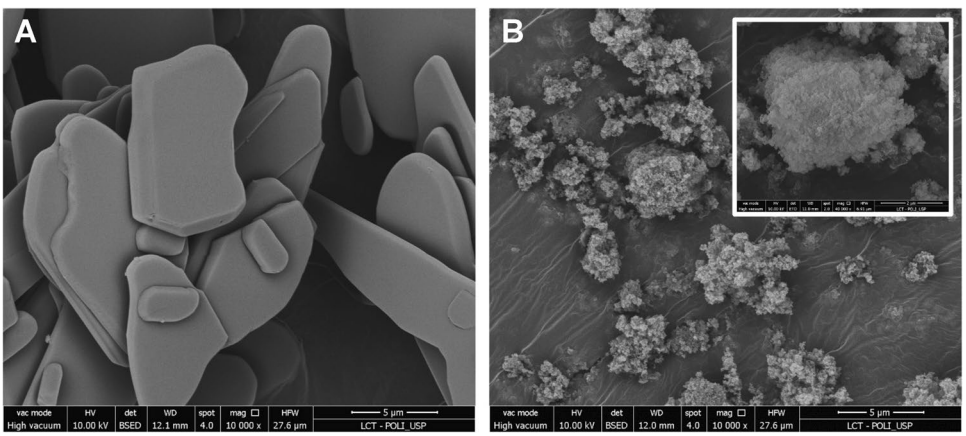

Fig. 1 Scanning electron micrographs of DCPD (**A**) and β-TCP (**B**) particles obtained using a back-scattered electron detector (BSED), at original magnification of 10,000×. An additional micrograph is presented for β-TCP particles at 40,000× original magnification obtained by secondary electrons (STD)

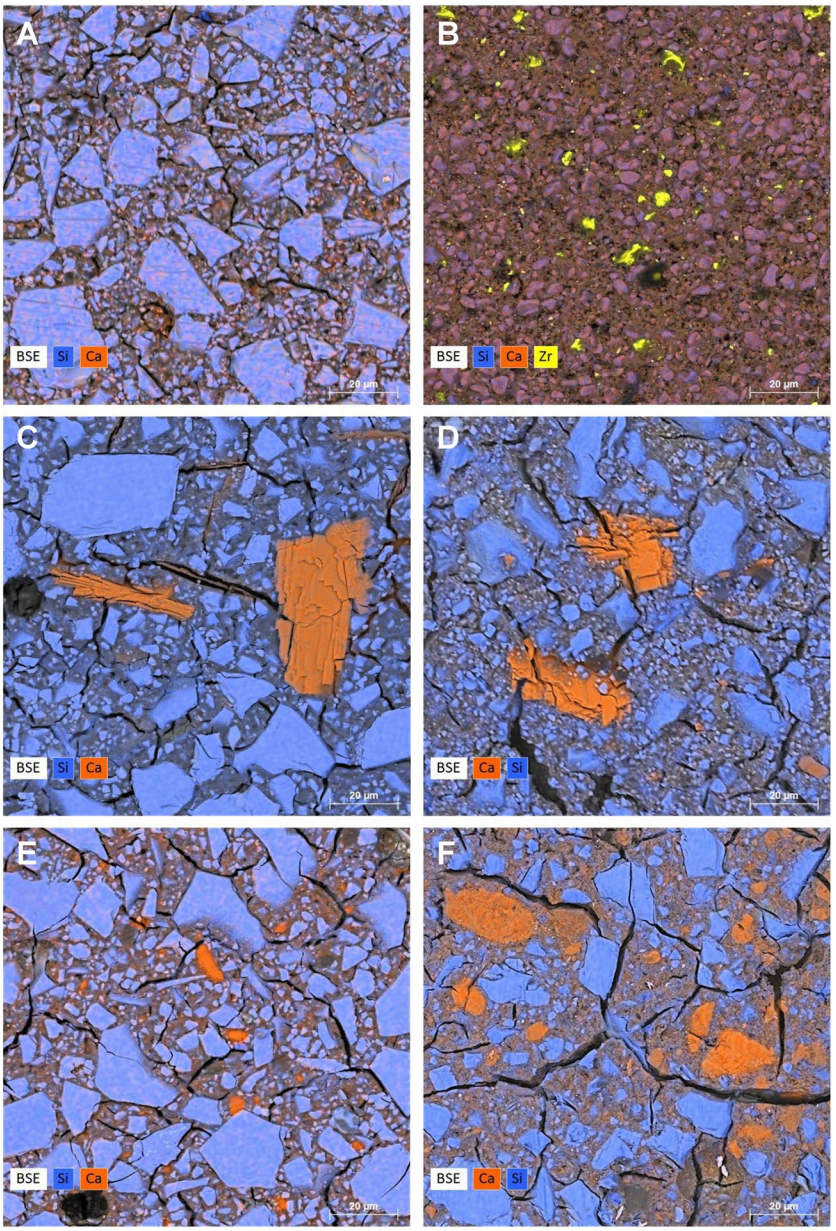

Fig. 2 Microstructure of the tested cements (**A** GIC, **B** CSC, **C** GIC + 5% DCPD, **D** GIC + 15% DCPD, **E** GIC + 5% β-TCP, **F** GIC + 15% β-TCP) observed under scanning electron microscopy using a back-scattered electron (BSE) detector, with calcium (in orange), silicon (in blue) and zirconium (in yellow) mapped using energy-dispersive X-ray spectroscopy (EDS)

Mineral:matrix ratio

Demineralized dentin samples had averages MMR between 2.4 and 6.9. After 56 days, with the exception of GIC + 15% DCPD, statistically significant increases in MMR were observed (between 4.4 and 6.9). However, no statistically significant differences were detected among the modified GICs and the two negative controls (composite and unmodified GIC, $p > 0.05$; Fig. 5). On the other hand, the dentin disks in contact with CSC showed a significant increase in MMR after 28 days, reaching a MMR of 65.4 after 56 days. This value exceeded the MMR of the sound dentin (30.9 ± 1.9).

Dentin hardness and elastic modulus (nanoindentation)

Nanoindentation test results are presented in Fig. 6. Hardness (kgf/cm^2) and elastic modulus (GPa) increased gradually from the lesion surface towards the sound dentin. Only samples in contact with CSC were statistically different from the other groups at all lesion depths for both properties ($p < 0.05$).

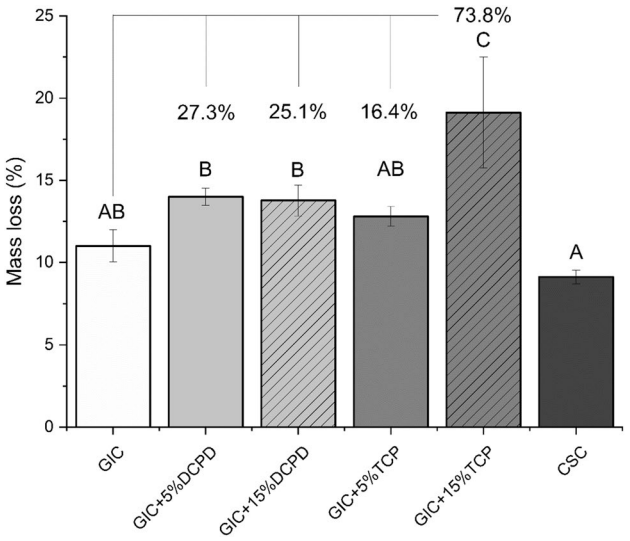

Fig. 3 Mass loss (%) after 7 days of immersion in deionized water. Error bars represent the standard deviation. Different uppercase letters indicate statistically significant differences among materials (one-way ANOVA/Tukey test). The increase in mass loss (in %) of experimental materials in relation to the unmodified GIC are presented at the top of the columns

Scanning electron microscopy

At the dentin surface, all groups show partial obliteration of the tubules, more pronounced for materials containing 15% DCPD or 15% β-TCP and for CSC (Fig. 7).

Transmission electron microscopy

Images of the interface between dentin and restorative material are shown in Fig. 8. For the "GIC" and "GIC + 5% β-TCP" groups, it was not possible to obtain sections for analysis. In all groups, apatite crystals close to the interface with the restorative material are observed. The dentin in contact with the composite showed shorter and thicker crystals compared to those found in dentin in contact with the modified GICs. The darker areas observed under GIC + 5% DCPD and GIC + 15% β-TCP indicate higher mineral content than the negative control. The highest mineral density was observed in dentin samples kept in contact with CSC. On the other hand, GIC + 15% DCPD resulted in less mineralized areas.

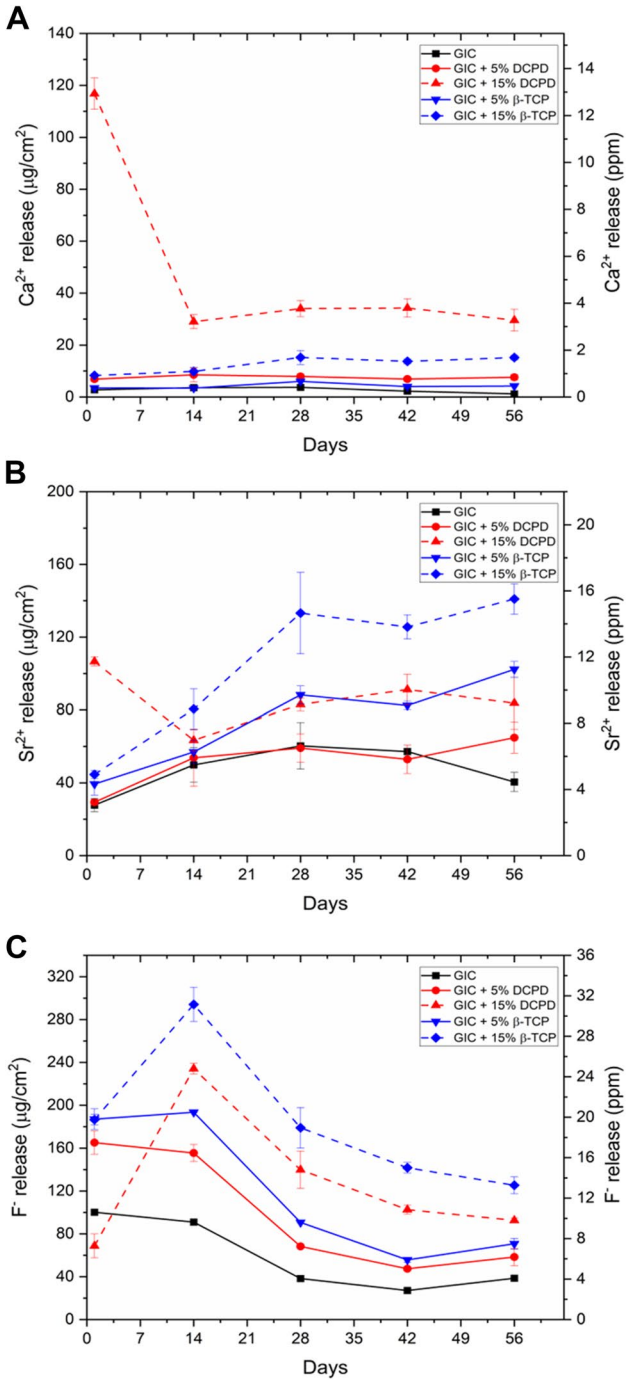

Fig. 4 Calcium (**A**), strontium (**B**), and fluoride (**C**) release in µg/cm^2 (left *y*-axis) and ppm (right *y*-axis) for the tested GICs. Error bars represent the standard deviation

Discussion

The aim of this study was to determine ion release, degradation, and remineralizing potential of a CSC and a GIC modified with DCPD or β-TCP particles. The glass particles in Fuji Gold Label 9 contain strontium rather than calcium in order to impart radiopacity to the cement. As such, Ca^{2+} release results of modified GICs can be attributed to the added CaP particles. Biodentine was chosen because of its indication as a long-term temporary restorative material. The replacement of a 5% fraction (by mass)

Table 1 Cumulative 56-day calcium, strontium, and fluoride release, in μg/cm^2

Cumulative ion release (μg/cm^2)			
	Ca^{2+}	Sr^{2+}	F^-
GIC	13.6 ± 1.6 ^{D}	235.7 ± 11.7 ^{D}	295.1 ± 1.1 ^{C}
GIC + 5% DCPD	37.9 ± 1.9 ^{C}	260.1 ± 6.7 ^{D}	494.5 ± 7.6 ^{B}
GIC + 5% β-TCP	21.2 ± 1.4 ^{D}	369.4 ± 5.1^{C}	597.6 ± 6.9 ^{B}
GIC + 15% DCPD	243.8 ± 8.5 ^{A}	428.0 ± 32.2 ^{B}	637.8 ± 9.2 ^{B}
GIC + 15% β-TCP	62.3 ± 0.2 ^{B}	525.0 ± 0.9 ^{A}	926.7 ± 37.2 ^{A}
CSC	4737.0 ± 735.9	-	-

For GICs, similar letters indicate absence of statistical difference (one-way ANOVA/Tukey test, $p > 0.05$)

of GIC glass by CaP was defined based on previous studies, in order to preserve GIC's strength [39]. The 15% fraction, though resulting in a material with reduced setting time and higher viscosity, was tested in order to verify if an increase in Ca^{2+} availability would increase dentin remineralization. All null hypotheses were rejected because (1) the experimental GICs showed higher ion release and degradation in water, (2) CSC showed higher calcium release than GIC (both modified and non-modified), and (3) CSC was the only material that promoted increases in dentin mineral content and mechanical properties.

The modified GICs presented higher degradation than the unmodified GIC. This finding is justified by the fact that the substitution of GIC glass by CaP particles changed the glass:liquid ratio defined by the manufacturer. The excess of poly(acrylic acid) increases glass dissolution, resulting in a higher polyacrylate salt matrix fraction in the final microstructure (as observed in Fig. 2),which facilitates the diffusion of fluids, increasing cement degradation [40]. In addition, there is a higher amount of unreacted carboxylic group, which increases water sorption [41]. Though a greater availability of calcium ions may favor the polyacrylate crosslinking [42–44] and reduce sorption and solubility, this effect was not observed.

CSC degradation was similar to that of the unmodified GIC. An in vitro study reported that Biodentine showed no mass loss after 28 days of immersion in HBSS [16]. Possibly, the difference in immersion media is responsible for the discrepant results. Deionized water promotes a faster dissolution of the cement, compared to ion-containing media. In addition, cement porosity, between 7.09 [45] and 13.44% [46] for Biodentine, would allow for transit of fluids through the material, favoring its degradation. In fact, an in vivo study reported a significant degradation of Biodentine after 6 months of clinical use [47].

The modified GICs presented higher ion release than the unmodified GIC, in agreement with previous reports [42, 48–50]. Similarly to what was described for mass loss in water, the lower glass:poly(acrylic acid) ratio in these materials results in an excess of acid, increasing particle dissolution and, consequently, ion release. The higher Ca^{2+} release found in DCPD-containing GIC in relation to β-TCP can be explained by the higher solubility of the former [51]. Furthermore, β-TCP synthesis procedure results in a partial substitution of calcium with magnesium, in order to

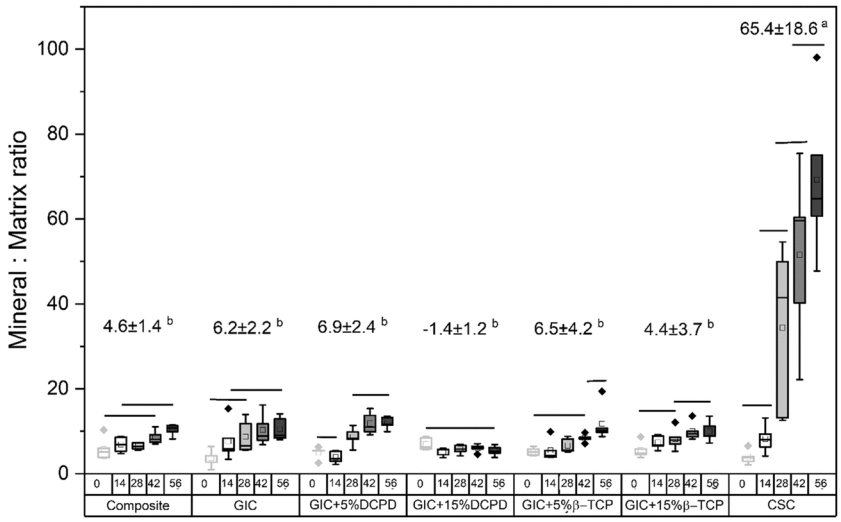

Fig. 5 Box plot showing the mineral-to-matrix ratio (MMR) results as a function of the material and the storage period (in days). In each box, the values for the first, second (median), and third quartile are represented. The square represents the average value for each experimental condition. The vertical lines indicate the minimum and maximum values and outliers are indicated by rhombuses. Horizontal lines above the boxes indicate absence of statistically significant differences among periods for the same material (repeated measures two-way ANOVA/Tukey test, $p < 0.05$). The numbers above the boxes indicate the variation in MMR between the demineralized dentin and after 56 days (one-way ANOVA/Tukey test, $p > 0.05$)

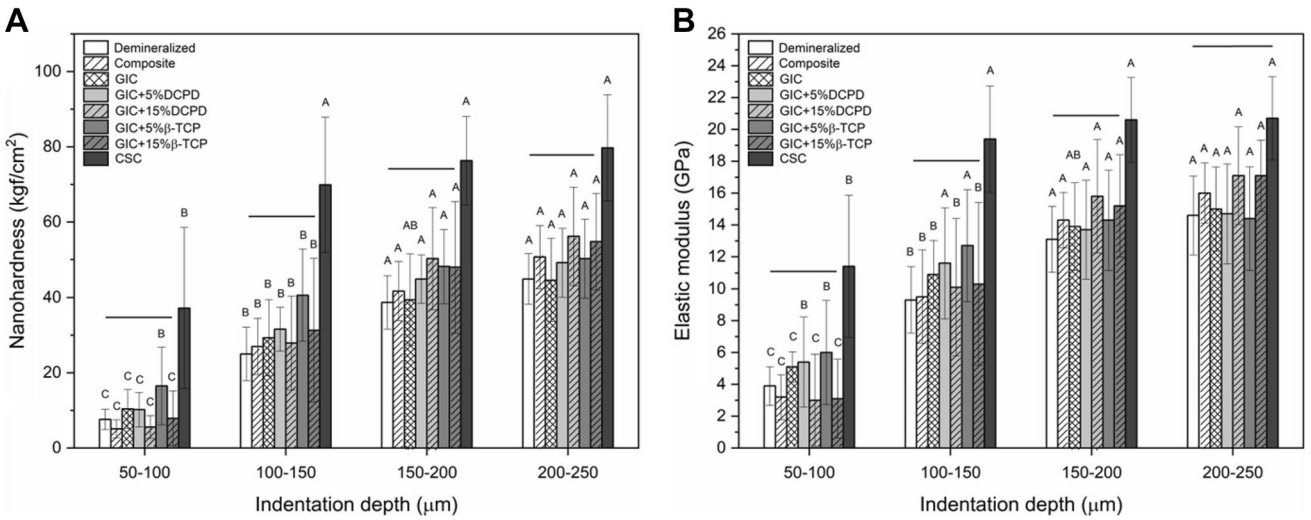

Fig. 6 Averages for nanohardness (**A**) and elastic modulus (**B**) at different lesion depths after 56 days in contact with the restorative materials. Error bars represent the standard deviation. Similar letters indicate the absence of statistically significant differences for the same material at different depths ($p < 0.05$). Lines above the columns indicate lack of statistically significant differences among materials for the same depth ($p < 0.05$)

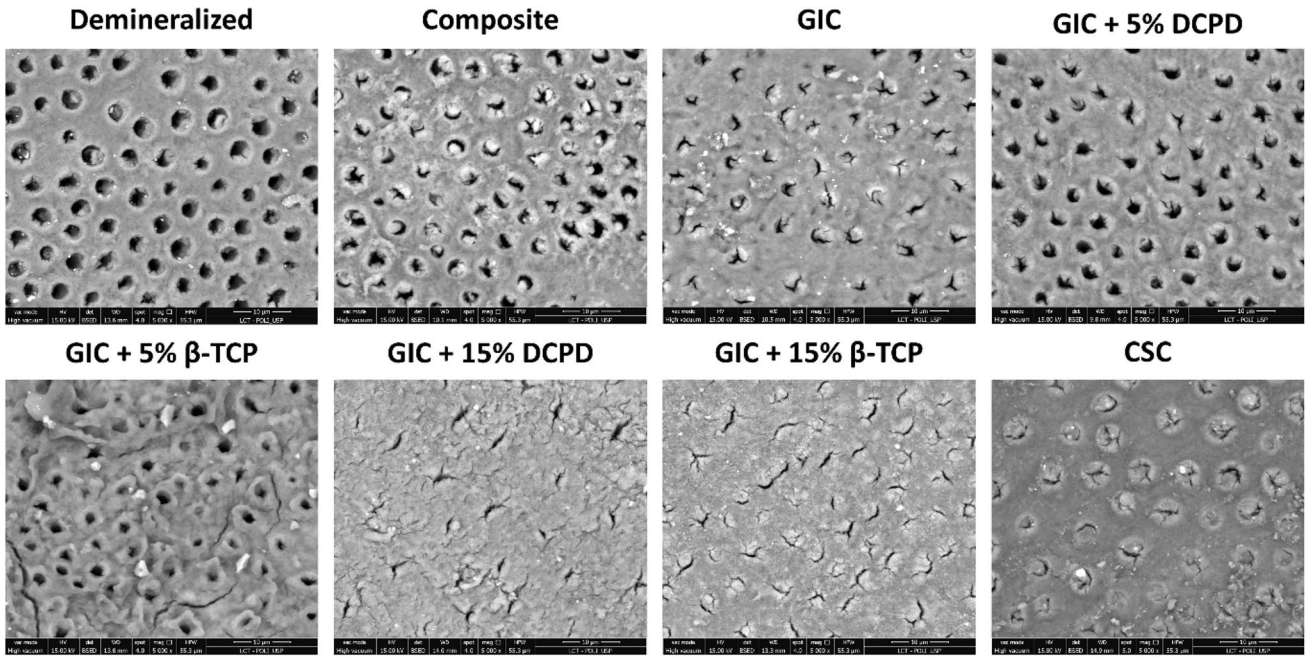

Fig. 7 Scanning electron microscope images of the dentin surface after contact with restorative materials for 56 days immersed in simulated body fluid (original magnification: 5000×)

stabilize the crystal and avoid its spontaneous transformation to hydroxyapatite [31]. The improved phase stability, however, reduces particle solubility. Among the modified GICs, GIC + 15% DCPD showed the highest Ca^{2+} release. Still, its cumulative release was much lower than that shown by the CSC, reflecting the later higher calcium content and higher particle surface area. The higher initial release of CSC is justified by the fact that, in the first hours, the transit of fluids (necessary for the hydration process) is more intense and decreases over time [52].

The significant increase in dentin MMR after 56 days of contact with the resin-based composite (negative control) is attributed to immersion in SBF, a solution containing high concentrations of calcium and phosphate (100.2 and

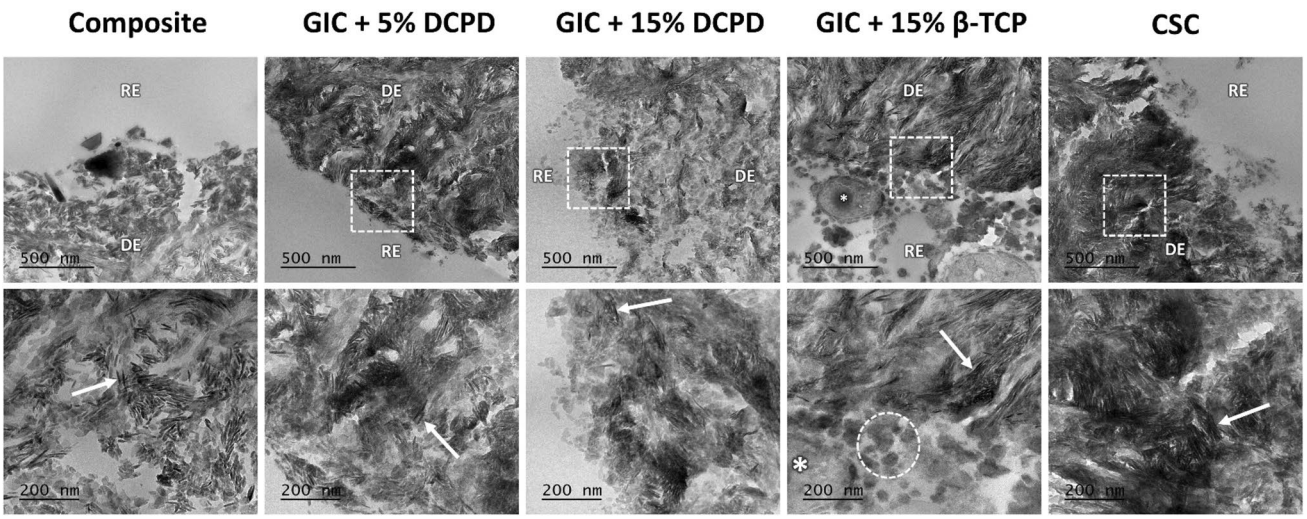

Fig. 8 Transmission electron microscope images of dentin samples after contact with restorative materials for 56 days. Top row images original magnification: 50,000×. With the exception of GIC + 15% β-TCP, restorative materials (RE) detached from the dentin sample (DE) during sectioning. The white squares indicate the areas shown at higher magnification (100,000×), presented at the bottom row. The arrows point to the crystals deposited after the restorative procedure. The asterisk indicates a glass particle after surface dissolution promoted by contact with polyacrylic acid, and the white circle, the β-TCP nanoparticles. Dentin samples restored with GIC and GIC + 5% β-TCP are not shown because it was not possible to obtain sections for observation

95.0 ppm, respectively), sufficient for mineral precipitation to occur [36]. The higher Ca^{2+} release from modified GICs was not enough to increase mineral precipitation at the demineralized dentin interface or to restore dentin mechanical properties compared to the unmodified GIC or the resin composite. In fact, a trend for reduced MMR of the samples kept in contact with GIC + 15% DCPD was observed, suggesting that the excess of poly(acrylic acid) may have caused additional demineralization, offsetting the higher Ca^{2+} availability. This hypothesis is confirmed by the sparse distribution of apatite crystals observed in the TEM images. Unfortunately, the absence of TEM images of demineralized dentin samples does not allow to affirm whether there was additional demineralization or absence of remineralization in the GIC + 15% DCPD group.

On the other hand, after 28 days in contact with CSC, dentin MMR reached values similar to sound dentin. Though particle morphology, size, and solubility may have contributed for CSC higher Ca^{2+} release, the remineralization results can be attributed to the calcium content in the final material, which is much higher for the CSC (55.4%) compared to other materials (up to 10.5% for modified GICs). Also, CSC releases OH^-, and the alkalinization of the medium favors apatite precipitation [53]. The greater density of apatite crystals observed in the TEM images is in agreement with the results of other studies [19, 54] and may justify the higher MMR than that of a sound dentin. In fact, only CSC was able to promote recovery of the mechanical properties of demineralized dentin across the entire lesion depth. The other groups showed no statistically significant differences in dentin elastic modulus or nanohardness in relation to demineralized dentin. There are three possible non-exclusive hypotheses to explain this finding: (1) insufficient Ca^{2+} release, (2) excess of poly(acrylic acid) leading to further demineralization, and (3) mineral deposition observed in the SEM images was restricted to the extrafibrillar area, which does not contribute to increase dentin mechanical properties [55]. There are very few studies comparing glass ionomer and calcium silicate cements in relation to their effectiveness on dentin remineralization, with different outcomes [19, 26–29]. Our results agree with those reporting a superior performance of CSC [19, 26, 27].

In summary, the results of the present study indicate that GIC, either unmodified or containing 5% or 15% of DCPD or β-TCP, is not capable of promoting dentin remineralization. Though the addition of calcium sources to GIC increased the Ca^{2+}, it was either insufficient or its effect was offset by the additional demineralization caused by higher acidity of the cement. On the other hand, the CSC was able to promote mineral precipitation and increase the mechanical properties of demineralized dentin.

Conclusion

All the null hypotheses were rejected. The addition of DCPD or β-TCP to GIC increased the release of Ca^{2+}, Sr^{2+}, and F^-. However, there were no statistically significant differences in mineral content and mechanical

properties of demineralized dentin between the GIC (with or without additional calcium sources) and the negative control (composite). On the other hand, the calcium silicate cement released much higher amounts of Ca^{2+} and was able to promote dentin remineralization.

Acknowledgements Author would like to thank Septodont for donating Biodentine.

Author contributions Handially S. Vilela: Investigation, Writing—original draft, review & editing. Rafael B. Trinca: Formal analysis. Tarsila V. M. Alves: Investigation. Taís S. Forlin: Investigation. Leticia O. Sakae: Investigation. Flávia S. Mariano: Investigation. Marcelo Giannini: Formal analysis. Flávia R. O. Silva: Investigation. Roberto R. Braga: Conceptualization, Supervision, Project administration, Formal analysis, Writing—review & editing.

Funding This study was funded by the São Paulo Research Foundation (FAPESP), grants 2020/12761–0, 2020/13983–6, and 2020/06313–4.

Declarations

Ethics approval and consent to participate The consent of the participants was written, as indicated and authorized by the Research Ethics Committee of the Faculty of Dentistry of the University of São Paulo (Number: 5.795.736 / CAAE: 39603020.5.0000.0075).

Competing interests The authors declare no competing interests.

References

1. Maltz M, Oliveira EF, Fontanella V, Carminatti G (2007) Deep caries lesions after incomplete dentine caries removal: 40-month follow-up study. Caries Res 41(6):493–496
2. Maltz M, Alves LS, Jardim JJ, Moura Mdos S, de Oliveira EF (2011) Incomplete caries removal in deep lesions: a 10-year prospective study. Am J Dent 24(4):211–214
3. Ribeiro CC, de Oliveira Lula EC, da Costa RC, Nunes AM (2012) Rationale for the partial removal of carious tissue in primary teeth. Pediatr Dent 34(1):39–41
4. Ricketts D, Lamont T, Innes NP, Kidd E, Clarkson JE (2013) Operative caries management in adults and children. Cochrane Database Syst Rev 28(3):CD003808
5. Schwendicke F, Dorfer CE, Paris S (2013) Incomplete caries removal: a systematic review and meta-analysis. J Dent Res 92(4):306–314
6. Li T, Zhai X, Song F, Zhu H (2018) Selective versus non-selective removal for dental caries: a systematic review and meta-analysis. Acta Odontol Scand 76(2):135–140
7. Mertz-Fairhurst EJ, Curtis JW Jr, Ergle JW, Rueggeberg FA, Adair SM (1998) Ultraconservative and cariostatic sealed restorations: results at year 10. J Am Dent Assoc 129(1):55–66
8. Corralo DJ, Maltz M (2013) Clinical and ultrastructural effects of different liners/restorative materials on deep carious dentin: a randomized clinical trial. Caries Res 47(3):243–250
9. Oz FD, Ergin E, Cakir FY, Gurgan S (2020) Clinical evaluation of a self-adhering flowable resin composite in minimally invasive class I cavities: 5-year results of a double blind randomized, controlled clinical trial. Acta Stomatol Croat 54(1):10–21
10. Paula AB, Laranjo M, Marto CM, Paulo S, Abrantes AM, Fernandes B et al (2020) Evaluation of dentinogenesis inducer biomaterials: an in vivo study. J Appl Oral Sci 28:e20190023
11. Okiji T, Yoshiba K (2009) Reparative dentinogenesis induced by mineral trioxide aggregate: a review from the biological and physicochemical points of view. Int J Dent 2009:464280
12. Gandolfi MG, Taddei P, Tinti A, Prati C (2010) Apatite-forming ability (bioactivity) of ProRoot MTA. Int Endod J 43(10):917–929
13. Parirokh M, Torabinejad M (2010) Mineral trioxide aggregate: a comprehensive literature review—Part I: chemical, physical, and antibacterial properties. J Endod 36(1):16–27
14. Gandolfi MG, Taddei P, Siboni F, Modena E, De Stefano ED, Prati C (2011) Biomimetic remineralization of human dentin using promising innovative calcium-silicate hybrid "smart" materials. Dent Mater 27(11):1055–1069
15. Camilleri J (2013) Investigation of Biodentine as dentine replacement material. J Dent 41(7):600–610
16. Grech L, Mallia B, Camilleri J (2013) Investigation of the physical properties of tricalcium silicate cement-based root-end filling materials. Dent Mater 29(2):e20–e28
17. Aboush YE, Torabzadeh H (2000) Clinical performance of Class II restorations in which resin composite is laminated over resin-modified glass-ionomer. Oper Dent 25(5):367–373
18. Kim YK, Yiu CK, Kim JR, Gu L, Kim SK, Weller RN et al (2010) Failure of a glass ionomer to remineralize apatite-depleted dentin. J Dent Res 89(3):230–235
19. Schwendicke F, Al-Abdi A, Pascual Moscardo A, Ferrando Cascales A, Sauro S (2019) Remineralization effects of conventional and experimental ion-releasing materials in chemically or bacterially-induced dentin caries lesions. Dent Mater 35(5):772–779
20. Hill R (2022) Glass ionomer polyalkenoate cements and related materials: past, present and future. Br Dent J 232(9):653–657
21. Zhao IS, Mei ML, Burrow MF, Lo EC, Chu CH (2017) Prevention of secondary caries using silver diamine fluoride treatment and casein phosphopeptide-amorphous calcium phosphate modified glass-ionomer cement. J Dent 57:38–44
22. Prabhakar AR, Paul MJ, Basappa N (2010) Comparative evaluation of the remineralizing effects and surface micro hardness of glass ionomer cements containing bioactive glass (S53P4): an in vitro study. Int J Clin Pediatr Dent 3(2):69–77
23. Yli-Urpo H, Narhi M, Narhi T (2005) Compound changes and tooth mineralization effects of glass ionomer cements containing bioactive glass (S53P4), an in vivo study. Biomaterials 26(30):5934–5941
24. Yli-Urpo H, Vallittu PK, Narhi TO, Forsback AP, Vakiparta M (2004) Release of silica, calcium, phosphorus, and fluoride from glass ionomer cement containing bioactive glass. J Biomater Appl 19(1):5–20
25. Valanezhad A, Odatsu T, Udoh K, Shiraishi T, Sawase T, Watanabe I (2016) Modification of resin modified glass ionomer cement by addition of bioactive glass nanoparticles. J Mater Sci Mater Med 27(1):3
26. Atmeh AR, Chong EZ, Richard G, Boyde A, Festy F, Watson TF (2015) Calcium silicate cement-induced remineralisation of totally demineralised dentine in comparison with glass ionomer cement: tetracycline labelling and two-photon fluorescence microscopy. J Microsc 257(2):151–160
27. Pires PM, Santos TP, Fonseca-Goncalves A, Pithon MM, Lopes RT, Neves AA (2018) Mineral density in carious dentine after treatment with calcium silicates and polyacrylic acid-based cements. Int Endod J 51(11):1292–1300
28. Neves AB, Bergstrom TG, Fonseca-Goncalves A, Dos Santos TMP, Lopes RT, de Almeida NA (2019) Mineral density changes in bovine carious dentin after treatment with bioactive

dental cements: a comparative micro-CT study. Clin Oral Investig 23(4):1865–1870
29. Zain S, Davis GR, Hill R, Anderson P, Baysan A (2020) Mineral exchange within restorative materials following incomplete carious lesion removal using 3D non-destructive XMT subtraction methodology. J Dent 99:103389
30. Trinca RB, Oliveira BA, Vilela HDS, Braga RR (2023) Effect of calcium orthophosphate particle size and CaP:glass ratio on optical, mechanical and physicochemical characteristics of experimental composites. Dent Mater 39(9):770–778
31. Viana IEL, Lopes RM, Silva FRO, Lima NB, Aranha ACC, Feitosa S et al (2020) Novel fluoride and stannous-functionalized beta-tricalcium phosphate nanoparticles for the management of dental erosion. J Dent 92:103263
32. Fridland M, Rosado R (2005) MTA solubility: a long term study. J Endod 31(5):376–379
33. Jingarwar MM, Pathak A, Bajwa NK, Sidhu HS (2014) Quantitative assessment of fluoride release and recharge ability of different restorative materials in different media: an in vitro study. J Clin Diagn Res 8(12):ZC31-4
34. Bezerra SJC, Viana IEL, Aoki IV, Duarte S, Hara AT, Scaramucci T (2022) In-vitro evaluation of the anti-cariogenic effect of a hybrid coating associated with encapsulated sodium fluoride and stannous chloride in nanoclays on enamel. J Appl Oral Sci 30:e20210643
35. Saeki K, Chien YC, Nonomura G, Chin AF, Habelitz S, Gower LB et al (2017) Recovery after PILP remineralization of dentin lesions created with two cariogenic acids. Arch Oral Biol 82:194–202
36. Kokubo T, Takadama H (2006) How useful is SBF in predicting in vivo bone bioactivity? Biomaterials 27(15):2907–2915
37. Sauro S, Osorio R, Watson TF, Toledano M (2015) Influence of phosphoproteins' biomimetic analogs on remineralization of mineral-depleted resin-dentin interfaces created with ion-releasing resin-based systems. Dent Mater 31(7):759–777
38. Bacino M, Girn V, Nurrohman H, Saeki K, Marshall SJ, Gower L et al (2019) Integrating the PILP-mineralization process into a restorative dental treatment. Dent Mater 35(1):53–63
39. Vilela HS, Resende MCA, Trinca RB, Scaramucci T, Sakae LO, Braga RR (2023) Glass ionomer cement with calcium-releasing particles: effect on dentin mineral content and mechanical properties. Dent Mater. https://doi.org/10.1016/j.dental.2023.11.005
40 Crisp S, Lewis BG, Wilson AD (1976) Characterization of glass-ionomer cements. 2. Effect of the powder: liquid ratio on the physical properties. J Dent 4(6):287–90
41. Begala AJ, Strauss UP (1972) Dilatometric studies of counterion binding by polycarboxylates. J Phys Chem-Us 76(2):254–0
42. Arita K, Lucas ME, Nishino M (2003) The effect of adding hydroxyapatite on the flexural strength of glass ionomer cement. Dent Mater J 22(2):126–136
43. Sharafeddin F, Karimi S, Jowkar Z (2019) Evaluation of the effect of micro-hydroxyapatite incorporation on the diametral tensile strength of glass ionomer cements. J Conserv Dent 22(3):266–269
44. Moshaverinia A, Ansari S, Moshaverinia M, Roohpour N, Darr JA, Rehman I (2008) Effects of incorporation of hydroxyapatite and fluoroapatite nanobioceramics into conventional glass ionomer cements (GIC). Acta Biomater 4(2):432–440
45. De Souza ET, Nunes Tameirao MD, Roter JM, De Assis JT, De Almeida NA, De-Deus GA (2013) Tridimensional quantitative porosity characterization of three set calcium silicate-based repair cements for endodontic use. Microsc Res Tech 76(10):1093–1098
46. Camilleri J, Grech L, Galea K, Keir D, Fenech M, Formosa L et al (2014) Porosity and root dentine to material interface assessment of calcium silicate-based root-end filling materials. Clin Oral Investig 18(5):1437–1446
47. Koubi G, Colon P, Franquin JC, Hartmann A, Richard G, Faure MO et al (2013) Clinical evaluation of the performance and safety of a new dentine substitute, Biodentine, in the restoration of posterior teeth — a prospective study. Clin Oral Investig 17(1):243–249
48. Chiu SY, Shinonaga Y, Abe Y, Harada K, Arita K (2017) Influence of porous spherical-shaped hydroxyapatite on mechanical strength and bioactive function of conventional glass ionomer cement. Materials (Basel) 10(1):27
49. Arita K, Yamamoto A, Shinonaga Y, Harada K, Abe Y, Nakagawa K et al (2011) Hydroxyapatite particle characteristics influence the enhancement of the mechanical and chemical properties of conventional restorative glass ionomer cement. Dent Mater J 30(5):672–683
50. Lucas ME, Arita K, Nishino M (2003) Toughness, bonding and fluoride-release properties of hydroxyapatite-added glass ionomer cement. Biomaterials 24(21):3787–3794
51. Dorozhkin SV (2011) Calcium orthophosphates: occurrence, properties, biomineralization, pathological calcification and biomimetic applications. Biomatter 1(2):121–164
52. Rajasekharan S, Martens LC, Cauwels R, Anthonappa RP, Verbeeck RMH (2021) Correction to: Biodentine material characteristics and clinical applications: a 3 year literature review and update. Eur Arch Paediatr Dent 22(2):307
53. Chen S, Mestres G, Lan W, Xia W, Engqvist H (2016) Cytotoxicity of modified glass ionomer cement on odontoblast cells. J Mater Sci Mater Med 27(7):116
54. Atmeh AR, Chong EZ, Richard G, Festy F, Watson TF (2012) Dentin-cement interfacial interaction: calcium silicates and polyalkenoates. J Dent Res 91(5):454–459
55. Bertassoni LE, Habelitz S, Kinney JH, Marshall SJ, Marshall GW Jr (2009) Biomechanical perspective on the remineralization of dentin. Caries Res 43(1):70–77

Publisher's Note Springer Nature remains neutral with regard to jurisdictional claims in published maps and institutional affiliations.

Springer Nature or its licensor (e.g. a society or other partner) holds exclusive rights to this article under a publishing agreement with the author(s) or other rightsholder(s); author self-archiving of the accepted manuscript version of this article is solely governed by the terms of such publishing agreement and applicable law.